Accurate Computation of the MGF of the Lognormal Distribution and its Application to Sum of Lognormals

C. Tellambura, *Senior Member, IEEE*, and D. Senaratne

***Abstract*—Sums of lognormal random variables (RVs) are of wide interest in wireless communications and other areas of science and engineering. Since the distribution of lognormal sums is not log-normal and does not have a closed-form analytical expression, many approximations and bounds have been developed. This paper develops two computational methods for the moment generating function (MGF) or the characteristic function (CHF) of a single lognormal RV. The first method uses classical complex integration techniques based on steepest-descent integration. The saddle point of the integrand is explicitly expressed by the Lambert function. The steepest-descent (optimal) contour and two closely-related closed-form contours are derived. A simple integration rule (e.g., the midpoint rule) along any of these contours computes the MGF/CHF with high accuracy. The second approach uses a variation on the trapezoidal rule due to Ooura and Mori. Importantly, the cumulative distribution function of lognormal sums is derived as an alternating series and convergence acceleration via the Epsilon algorithm is used to reduce, in some cases, the computational load by a factor of 10^6! Overall, accuracy levels of 13 to 15 significant digits are readily achievable.**

***Index Terms*—Sum of lognormals, moment-generating function, characteristic function.**

I. Introduction

THE lognormal distribution is widely used in various branches of science and engineering [1]–[3]. In wireless communications, it is used to model large-scale signal fading and co-channel interference for cellular mobile networks, ultra-wide band systems and other wireless networks [4]–[10]. Closed-form exact analytical expressions for the lognormal characteristic function (CHF), the moment generating function (MGF), and the distribution function of a sum of independent lognormal random variables (RVs) are not available. Wireless researchers have attacked the famous sum of lognormals (SLN) problem for decades starting with [11]–[15].

Previous SLN studies may broadly be classified into two categories.

I. The first category approximates the SLN distribution by another lognormal one (whose parameters are determined by moment or cumulant matching techniques). For example, Fenton [11] approximates based on the first and second moments (as well as the third- and fourth-order moments), while Schleher [13] uses Gram-Charlier series based on cumulant matching. Schwartz-Yeh [12], Wilkinson [12] and Farley [12] also use moment matching. Other examples include negative moment matching [16]; generalized moment matching [6], [7], [16] and MGF matching [17]. Some of these approaches have been extended for correlated lognormal sums as well [17], [18].

II. Although the lognormal cumulative distribution function (CDF) is a straight line on a lognormal paper [11], the SLN CDF is not. Therefore, the above approximations are not globally accurate [19], [20]. The second category of approximations thus involves representing the SLN distribution by a distribution other than the lognormal distribution. For example, the SLN distribution is approximated by power lognormal and generalized lognormal distributions [21]–[23], Log-shifted Gamma distribution [24], [25], and Type-IV Pearson distribution [26]. References [27], [28] use linear and quadratic estimates with regression analysis.

The main difficulties of numerical integration for the lognormal MGF/CHF are the oscillations and the slow decay rate of the integrand. Perhaps because of these drawbacks direct numerical methods have not been investigated much, except by Beaulieu and Xie [29]. They investigated the Simpson's rule, the trapezoidal rule and Hermite polynomials and settled on the modified Clenshaw-Curtis rule.

To overcome these problems, we first develop two highly accurate numerical methods.

I. The first one uses complex contour integration techniques [30]. The idea is to deform the lognormal MGF/CHF integral via Cauchy's theorem. Exploiting this idea, Gubner [31] suggested integrating along a contour parallel to the x-axis so as to reduce the oscillatory nature of the integrand; however this contour is not the best. The best contour ensures a fast decay rate and removes oscillations of the integrand completely. The steepest-descent constant-phase contour, which passes through the saddle point of the integrand, have these properties. Interestingly, a part of this optimal contour coincides with the Gubner's contour [31]. We express the saddle point by using the Lambert function $\mathcal{W}(x)$ [32]. Because the optimal contour is not closed-form, we derive two closely-related closed-form contours. A simple integration rule (e.g., the

Paper approved by R. K. Mallik, the Editor for Diversity and Fading Channels of the IEEE Communications Society. Manuscript received December 10, 2008; revised June 11, 2009 and August 14, 2009.

The authors are with the Department of Electrical and Computer Engineering, University of Alberta, Edmonton, AB T6G 2V4, Canada (e-mail: {chintha, damith}@ece.ualberta.ca).

Digital Object Identifier 10.1109/TCOMM.2010.05.080640

midpoint rule) along any of these contours computes the MGF/CHF with extremely high precision.

II. The second approach utilizes the trapezoidal rule to compute the lognormal CHF. The trapezoidal rule is very efficient, and the error decreases exponentially when the integrand is analytic and bounded in a strip around the real axis [30]. However, direct application of the trapezoidal rule fails in this case, as has been observed in [29]. We employ an ingenious transformation proposed by Ooura and Mori [33], which enables the use of the trapezoidal rule to derive a highly accurate, efficient formula for the lognormal CHF.

Given the MGF/CHF, numerical integration is further required to compute the SLN CDF. We develop an efficient and accurate method based on Longman [34], [35]. His idea is to break down a highly oscillating infinite integral, say, $\int_0^\infty f(x)dx$ into a series of finite integrals $\int_{x_k}^{x_{k+1}} f(x)dx$, where x_k and x_{k+1} are two consecutive zeros of $f(x)$. Consequently, the integral is expressed as an alternating series whose individual terms can be readily evaluated by using simple numerical methods. Using this approach, we derive the SLN CDF as an alternating series. However, since the number of terms can sometimes be as high as 10^6 or more, Longman [34], [35] originally used convergence acceleration based on the Euler algorithm. However, the more powerful Epsilon algorithm [36], [37] is used in this paper. This acceleration method achieves remarkable computational efficiencies on the order of 10^6.

The paper is organized as follows: Section II provides the background. Section III develops the lognormal MGF/CHF computation based on contour integration. The Ooura-Mori based method is developed in Section IV. In Section V we discuss the SLN CDF problem. Numerical results follow in Section VI. Section VII concludes the paper.

Notation: The imaginary unit $\mathrm{j} = \sqrt{-1}$. For complex z, z^* is the conjugate; $\arg(z)$, the argument; $|z|$, the magnitude; $\Re(z)$, the real part; $\Im(z)$, the imaginary part. $\mathbb{E}[\cdot]$ is the expected value. The derivative of $g(z)$ is $g'(z)$. $\mathbb{R}$ and $\mathbb{C}$ are the sets of real and complex numbers. The CDF, CHF and MGF of a random variable Y are denoted by $F_Y(.)$, $\Phi_Y(.)$ and $\mathcal{M}_Y(.)$, respectively.

II. Basics

A. Lognormal distribution

If $X \sim \mathcal{N}(\mu, \sigma^2)$ is a Gaussian RV with mean μ and variance σ^2, then $Y = \mathrm{e}^X$ is a lognormal random variable. In wireless communications, X represents a signal power level with its mean and the variance expressed in dB units. In this case, $\mu = \xi\mu_{\mathrm{dB}}$, and $\sigma^2 = \xi^2\sigma^2_{\mathrm{dB}}$, where $\xi = \frac{\ln(10)}{10} = 0.2303$.

The MGF of the lognormal distribution is given by

$$\mathcal{M}(s) = \mathbb{E}\left[\mathrm{e}^{-sY}\right] = \int_{-\infty}^{\infty} \mathrm{e}^{-s\mathrm{e}^t} \frac{\mathrm{e}^{-\frac{1}{2}\left(\frac{t}{\sigma}\right)^2}}{\sqrt{2\pi\sigma^2}}\,\mathrm{d}t,\ \Re(s) \geq 0. \tag{1}$$

The MGF exists for all $\alpha \geq 0$ in the right half of the complex $s = \alpha + \mathrm{j}\omega$ plane; and the special case $\alpha = 0$ yields the CHF. Since $\mathcal{M}(s^*) = (\mathcal{M}(s))^*$, we focus, without any loss of generality, only on the case $\omega \leq 0$. Furthermore, we assume a zero mean for X without loss of generality, because $\mathbb{E}\left[\mathrm{e}^{-s\mathrm{e}^{X+\mu}}\right] = \mathcal{M}(s\mathrm{e}^{\mu})$. Although the MGF is customarily defined as $\mathbb{E}\left[\mathrm{e}^{sY}\right]$, the definition $\mathbb{E}\left[\mathrm{e}^{-sY}\right]$, which is the Laplace transform of the probability density function, is employed throughout the paper.

The lognormal CHF is given by

$$\Phi(\omega) = \mathbb{E}\left[\mathrm{e}^{\mathrm{j}\omega Y}\right] = \int_{-\infty}^{\infty} \mathrm{e}^{\mathrm{j}\omega\mathrm{e}^t} \frac{1}{\sqrt{2\pi\sigma^2}} \mathrm{e}^{-\frac{1}{2}\left(\frac{t}{\sigma}\right)^2}\,\mathrm{d}t. \tag{2}$$

This equation (2) is a special case of the MGF with $\Phi(\omega) = \mathcal{M}(-\mathrm{j}\omega)$.

B. Contour integration

Consider a complex function $f(z) = u(x,y) + \mathrm{j}\,v(x,y)$ of complex $z = x + \mathrm{j}\,y$, where $x, y, u(x,y), v(x,y) \in \mathbb{R}$. If the Cauchy-Riemann conditions [38, 3.7.30] are satisfied, $f(z)$ is **analytic**. In this case, the gradients of $u(x,y)$ and $v(x,y)$ are orthogonal. That is, the contour lines $u(x,y) = C_u$ are orthogonal to contour lines $v(x,y) = C_v$ for all constants $C_u, C_v \in \mathbb{R}$. If $f(z)$ is analytic in the neighborhood of z_0 and $f'(z_0) = 0$, then $z_0 = x_0 + \mathrm{j}\,y_0$ is called a **saddle point** of $f(z)$. This name arises because the contours of $u(x,y)$ and $v(x,y)$ have valleys and hills in orthogonal directions in the neighborhood of this point, such that the surface bears the shape of a 'saddle'. The contour (path) that passes through this point satisfying $v(x,y) = v(x_0,y_0)$ is called the **steepest descent** contour for $u(x,y)$ [39].

Such contours are useful when we consider integrals of the form

$$I = \int_{\mathcal{C}} \mathrm{e}^{-\lambda f(z)}\,\mathrm{d}z, \tag{3}$$

where $\mathcal{C}$ is a contour in the complex plane. Cauchy's theorem tells that for analytic integrands, the integral remains fixed for a wide class of contours. Thus, $\mathcal{C}$ can be chosen to be a contour on which $v(x,y)$ remains constant, which eliminates the oscillations completely! The contribution of the integrand along this contour would be all in-phase, and therefore, add coherently. Moreover, since it passes through the saddle point z_0 of $f(z)$, it is the steepest descent contour for $\Re(f(z))$ (i.e., the magnitude $\left|e^{-\lambda f(z)}\right|$ of the integrand decays the fastest).

Steepest-descent contours are often used to derive asymptotic value as $\lambda \to \infty$ [39]. The idea of using these for numerical evaluation, as opposed to asymptotic expansions, is not new either. References [30], [40], [41] use this idea for numerical computations. However, the use of this idea to compute the lognormal MGF/CHF appears to be new.

In sum, the steepest-descent contour $\mathcal{L}$ is given by the constant-phase condition:

$$\mathcal{L} = \{x + \mathrm{j}\,y |\ v(x,y) = v(x_0,y_0)\}. \tag{4}$$

Along this contour, the integral (3) becomes

$$I = \mathrm{e}^{-\mathrm{j}\,\lambda v(x_0,y_0)} \int_{\mathcal{L}} \mathrm{e}^{-\lambda u(x,y)}\,\mathrm{d}z. \tag{5}$$

Note the two main advantages of integrating along $\mathcal{L}$:

I. The oscillations in the integrand, due to the $\lambda\mathrm{j}\,v(x,y)$ term in the exponent, are eliminated.

II. The integrand exhibits the fastest rate of decay, as the integration moves away from the saddle point z_0 along the contour $\mathcal{L}$. Often this decay rate is exponential.

These properties greatly facilitate the use of simple numerical integration methods with high accuracy.

III. Computation of the MGF (Contour Integration)

A. Saddle point

We can readily show that the integrand of (1) satisfies the Cauchy-Riemann conditions and is analytic. Therefore, the integration path along the real axis can be deformed to obtain a more desirable contour $\mathcal{L}$ on the complex plane. Thus, the MGF can be written as

$$\mathcal{M}(s) = c \int_{\mathcal{L}} \mathrm{e}^{-\lambda\varphi(z)}\,\mathrm{d}z, \tag{6}$$

where $c = \frac{1}{\sqrt{2\pi\sigma^2}}$, $\lambda = 1/\sigma^2$, $\zeta = s\sigma^2$, $\varphi(z) = \zeta\mathrm{e}^z + \frac{z^2}{2}$, and $\mathcal{L}$ is a constant-phase contour to be determined later. As mentioned before, the saddle point is required for this contour. Since the saddle point z_0 satisfies $\varphi'(z_0) = \zeta\mathrm{e}^{z_0} + z_0 = 0$, it can be explicitly given by

$$z_0 = -\mathcal{W}(\zeta) \tag{7}$$

where $\mathcal{W}(.)$ is the *Lambert W function*, which is defined via $\mathcal{W}(z)\,\mathrm{e}^{\mathcal{W}(z)} = z$. It is real for $z \in \mathbb{R}$ and $z \geq \frac{1}{\mathrm{e}}$. Arbitrary-precision complex floating point evaluation of $\mathcal{W}(z)$ for all $z \in \mathbb{C}$ is possible with common software such as Maple, Mathematica and MATLAB. A comprehensive discussion of the properties of the Lambert function can be found in [32].

B. Steepest descent constant-phase contour

Let $\varphi(z_0) = C_0 + \mathrm{j}\,C_1$. The derivative $\frac{\mathrm{d}}{\mathrm{d}z}\varphi(z) = \varphi'(z) = \zeta\mathrm{e}^z + z$ is given by

$$\begin{aligned}\varphi'(z) &= \zeta\mathrm{e}^{x+\mathrm{j}\,y} + (x+\mathrm{j}\,y)\\ &= |\zeta|\,\mathrm{e}^x\cos(y+\theta) + x + \mathrm{j}\left(|\zeta|\,\mathrm{e}^x\sin(y+\theta) + y\right),\end{aligned} \tag{8}$$

where $\theta = \arg(\zeta) = \arg(s) = \tan^{-1}\left(\frac{\omega}{\alpha}\right)$. The relationship between C_0 and C_1 can be determined, by setting (8) to zero.

We expand $\varphi(z)$ first, in order to describe the steepest-descent constant-phase contour. By using $z = x + \mathrm{j}\,y$ and $s = \alpha + \mathrm{j}\,\omega$ the exponent can be expressed as

$$\begin{aligned}\varphi(z) &= \Re(\varphi(z)) + \mathrm{j}\,\Im(\varphi(z)) = (\alpha+\mathrm{j}\,\omega)\sigma^2\mathrm{e}^{x+\mathrm{j}\,y} + \frac{(x+\mathrm{j}\,y)^2}{2}\\ &= \mathrm{e}^x\left(\alpha\cos(y) - \omega\sin(y)\sigma^2 + \frac{x^2-y^2}{2}\right)\\ &\qquad + \mathrm{j}\,\mathrm{e}^x\left(\alpha\sin(y) + \omega\cos(y)\sigma^2 + xy\right)\\ &= \left(|\zeta|\,\mathrm{e}^x\cos(y+\theta) + \left(\frac{x^2-y^2}{2}\right)\right)\\ &\qquad + \mathrm{j}\,\left(|\zeta|\,\mathrm{e}^x\sin(y+\theta) + xy\right).\end{aligned} \tag{9}$$

By using the constant phase condition (4) and (9), we obtain the steepest-descent contour as

$$\mathcal{L} = \left\{x + \mathrm{j}\,y \,\middle|\, |\zeta|\,\mathrm{e}^x\sin(y+\theta) + xy = C_1\right\}. \tag{10}$$

Since (x_0, y_0) satisfies (10), this contour $\mathcal{L}$ passes through the saddle point. $\mathcal{L}$ can be shown to lie in the range $-\infty < x < \infty$ and $0 \leq y \leq -\theta$. Moreover, the derivative $\frac{\mathrm{d}y}{\mathrm{d}x}$ along the contour $\mathcal{L}$ can be computed from (10) to be

$$\frac{\mathrm{d}y}{\mathrm{d}x} = -\frac{|\zeta|\,\mathrm{e}^x\sin(y+\theta) + y}{|\zeta|\,\mathrm{e}^x\cos(y+\theta) + x}. \tag{11}$$

Although (10) and (11) supply what is needed for the problem at hand, two more points must be clarified here.

I. First, we note that the contour (10) is not resolvable such that y is expressed as a closed-form function of x. Although, x can be obtained as a function of y, integrating over y is not desired (Subsection III-C). Thus, for a given x, $y \in \mathcal{L}$ must be determined numerically. This determination is not too difficult because we know that $y \in [0, -\theta]$ for all x. Consequently, a simple bisection search can be used to determine y for each x. Although the bisection method is fail-proof, it has only a linear convergence rate, requiring a large number of iterations. Since the derivative is explicitly known (11), a much better alternative is the Newton-Raphson method, which has a quadratic convergence rate [42]. However, since the derivative tends to be unstable (see below) near the saddle point z_0, so does the Newton-Raphson method. Therefore, we adopted a hybrid strategy whereby the bisection method is used only when $|x - x_0| \leq \epsilon$ (ϵ is a small number). Otherwise, the Newton-method is used to determine y for given x. The hybrid strategy was found to be about 100 times faster than the simple bisection method.

II. The second difficulty is that both the numerator and denominator of (11) approach zero at the saddle point (x_0, y_0). This finding is not surprising because (8) shows that the derivative is the ratio between the real and imaginary parts of $\varphi'(z)$. Thus, the derivative at the saddle point is given by a limiting process, which can be evaluated by using the *L'Hospital's rule*. It can be shown that

$$\left.\frac{\mathrm{d}y}{\mathrm{d}x}\right|_{\substack{x=x_0\\y=y_0}} = \sqrt{\frac{(1-x_0)^2}{y_0^2} + 1} - \left(\frac{1-x_0}{y_0}\right). \tag{12}$$

C. Numerical evaluation

Now we are in a position to evaluate the MGF via the complex integral (6) and the contour (10). When integrating over the contour $\mathcal{L}$, either x or y can be taken as the independent variable. However, the upper limit of y is dependent on the argument of $\mathcal{M}(s)$, whereas the limits of x are not. Moreover, when s is real, the limit of y is zero; i.e., the optimal contour is simply the real axis. For these reasons, we use x as the independent variable. Since $\mathrm{d}z = \mathrm{d}x + \mathrm{j}\,\mathrm{d}y = \left(1 + \mathrm{j}\,\frac{\mathrm{d}y}{\mathrm{d}x}\right)\mathrm{d}x$, the MGF (10) is given by

$$\begin{aligned}\mathcal{M}(s) = c\mathrm{e}^{-\mathrm{j}\,\lambda C_1}\int_{-\infty}^{\infty} &\mathrm{e}^{-\lambda\left(|\zeta|\mathrm{e}^x\cos(y+\theta) + \frac{x^2-y^2}{2}\right)}\\ &\left(1 - \mathrm{j}\,\frac{|\zeta|\,\mathrm{e}^x\sin(y+\theta) + y}{|\zeta|\,\mathrm{e}^x\cos(y+\theta) + x}\right)\mathrm{d}x,\end{aligned} \tag{13}$$

where y is a function of x governed by (10) for each $z = x + \mathrm{j}\,y \in \mathcal{L}$. We note that the main contribution to the integral

occurs near the saddle point $x = x_0$. Thus, we substitute $\sqrt{\frac{\lambda}{2}}(x - x_0) = t$ to obtain

$$\mathcal{M}(s) = \frac{\mathrm{e}^{-\mathrm{j}\,\lambda C_1}}{\sqrt{\pi}} \int_{-\infty}^{\infty} \mathrm{e}^{-t^2} q(t)\,\mathrm{d}t, \tag{14}$$

where

$$q(t) = \mathrm{e}^{-\lambda\left(|\zeta|\mathrm{e}^{\tilde{\sigma}t+x_0}\cos(y+\theta)+\frac{x_0^2+2\tilde{\sigma}x_0t-y^2}{2}\right)} \left(1 - \mathrm{j}\,\frac{|\zeta|\,\mathrm{e}^{\tilde{\sigma}t+x_0}\sin(y+\theta)+y}{|\zeta|\,\mathrm{e}^{\tilde{\sigma}t+x_0}\cos(y+\theta)+\tilde{\sigma}t+x_0}\right), \tag{15}$$

$\tilde{\sigma} = \sqrt{2}\sigma$, and y is given by (10) with $x = \tilde{\sigma}t + x_0$. The MGF can now be evaluated by using a simple mid-point rule as follows:

$$\mathcal{M}(s) = \frac{h\mathrm{e}^{-\mathrm{j}\,\lambda C_1}}{\sqrt{\pi}} \sum_{k=-\infty}^{\infty} \mathrm{e}^{-k^2h^2} q(kh + h/2) + E_h, \tag{16}$$

where the error term E_h rapidly decays with decreasing h. This computation requires three simple steps:

I Calculate the saddle point z_0 by using (7).
II Solve $y = y_k$ in (10) for $x = x_k = \tilde{\sigma}(kh + h/2) + x_0$.
III Sum (16) to the required precision.

This computational method has high accuracy. For example, the lognormal CDF can be calculated at about 15-digit accuracy (i.e., an error less than 10^{-15}) by inverting the CHF on MATLAB which has a typical accuracy level of 2.2×10^{-16}. Further details are found in Section VI.

Nevertheless, the above approach requires the numerical computation of the steepest-descent contour $\mathcal{L}$ (10). Evaluation can be greatly improved if $\mathcal{L}$ can be replaced with a contour along which y is given as a function of x in closed-form (i.e., $y = y(x)$). The replacement contour must be as close as possible to $\mathcal{L}$ in order to retain the twin benefits of reduced oscillations and the fastest rate of decay. We therefore impose several constraints on the replacement contour: (i.) it must pass through the saddle point z_0, (ii.) it must have the same slope $\frac{\mathrm{d}y}{\mathrm{d}x}$ on the saddle point as (12), (iii.) it must have the same limits as $\mathcal{L}$ when $x \to \pm\infty$. In the following, we develop closed-from 'atan' and 'tanh' contours that satisfy these conditions.

D. Atan contour

This closed-form contour is defined by

$$\mathcal{L}_1 : y(x) = -\frac{\theta}{\pi}\tan^{-1}(ax + b) - \frac{\theta}{2}, \tag{17}$$

where $x = \Re(z), y = \Im(z), \theta = \arg(s) < 0$. The case $\theta = 0$ corresponds to when the argument of $\mathcal{M}(s)$ is completely real, and, in this case, the steepest-descent contour $\mathcal{L}$ is the real axis. The parameters $a, b \in \mathbb{R}$ are to be estimated such that

- $\mathcal{L}_1$ passes through the saddle point $z_0 = x_0 + \mathrm{j}y_0 = -\mathcal{W}(s\sigma^2)$.
- $\mathcal{L}_1$ has the same derivative $\frac{\mathrm{d}}{\mathrm{d}x}y(x)\big|_{(x_0,y_0)} = y'(x_0)$ as (12).

These conditions translate to

$$ax_0 + b = -\tan\left(\frac{\pi}{\theta}\left(y_0 + \frac{\theta}{2}\right)\right) = \cot\left(\frac{\pi y_0}{\theta}\right)$$

$$y'(x_0) = \varphi = \frac{-a\theta}{\pi\left(1 + (ax_0 + b)^2\right)} = -\frac{a\theta}{\pi}\sin^2\left(\frac{\pi y_0}{\theta}\right),$$

where $\varphi = \frac{y_0}{\sqrt{(1-x_0)^2+y_0^2}+(1-x_0)}$.

Solving for a and b, one gets

$$a = \frac{-\frac{\pi\varphi}{\theta}}{\sin^2\left(\frac{\pi y_0}{\theta}\right)}, \quad \text{and} \quad b = -ax_0 + \cot\left(\frac{\pi y_0}{\theta}\right).$$

The parameters a and b can always be uniquely determined given that $0 < y_0 < -\theta \le \frac{\pi}{2}$ for all s. Derivative $y'(.)$ is given by

$$y'(x) = -\frac{a\theta}{\pi}\sin^2\left(\frac{\pi y(x)}{\theta}\right). \tag{18}$$

This contour $\mathcal{L}_1$ can now be used in (6) to obtain

$$\mathcal{M}(s) = c\int_{-\infty}^{\infty} \mathrm{e}^{-\lambda\varphi(x+\mathrm{j}\,y(x))}(1 + \mathrm{j}\,y'(x))\,\mathrm{d}x. \tag{19}$$

Again, this integrand has virtually no oscillations and decays rapidly. Therefore, a simple trapezoidal rule or midpoint rule can be used to evaluate the integral.

Note that due to the conjugate symmetry of $\mathcal{M}(s)$, it is sufficient to be able to evaluate $\mathcal{M}(s)$ for $\Im(s) < 0$.

E. Tanh contour

Alternatively, a hyperbolic tangent contour given by

$$\mathcal{L}_2 : y(x) = -\frac{\theta}{2}\tanh(ax + b) - \frac{\theta}{2} \tag{20}$$

may be used. Parameters a and b can be derived as before to be

$$a = \frac{\varphi}{2y_0\left(1 + \frac{y_0}{\theta}\right)}, \quad \text{and} \quad b = -\tanh^{-1}\left(\frac{2y_0}{\theta} + 1\right) - ax_0.$$

The derivative along $\mathcal{L}_2$ is given by

$$y'(x) = -\frac{a\theta}{2}\mathrm{sech}^2(ax + b) = 2ay(x)\left(1 + \frac{y(x)}{\theta}\right).$$

With this contour, the MGF can be expressed similar to (19).

The accuracy and numerical efficiencies of the steepest-descent contour, the 'atan contour' and the 'tanh contour' are discussed in Section VI.

IV. An Alternate Approach to Steepest Descent Contours: The Ooura-Mori Method

Here we take a different approach to tackle the same problem. Before describing this method, we will explain the motivation. The integral

$$I = \int_{-\infty}^{\infty} F(x)\,\mathrm{d}x$$

can be approximated by its trapezoidal sum,

$$I(h) = h\sum_{k=-\infty}^{\infty} F(kh),$$

where $h > 0$ is the step size. The trapezoidal rule is very efficient, and the error decreases exponentially (i.e., $|I - I(h)| \sim O(\mathrm{e}^{-2\pi\alpha/h})$ as $h \to 0$ for some $\alpha > 0$) when the integrand is analytic and bounded in a strip around the real axis [30]. However, the truncation of the infinite sum $I(h)$ results in a truncation error if the integrand decays slowly. For instance, the truncation error is not small if $F(x) \sim O(|x|^{-\alpha})$ only as $x \to \pm\infty$, but becomes negligibly small if $F(x) \sim O(\mathrm{e}^{-\alpha|x|})$ as $x \to \pm\infty$. Thus, the fundamental requirement for the trapezoidal rule to be accurate is that $F(kh)$ must rapidly decay to zero as $|k| \to \infty$. The Ooura-Mori method [33] is an ingenious transformation to ensure rapid decay rate of the integrand.

For simplicity, we consider only the CHF case here. By substituting $\mathrm{e}^t = x$ in (2), we find that

$$\Phi(\omega) = \int_0^\infty f(x)\cos(\omega x)\,\mathrm{d}x + \mathrm{j}\int_0^\infty f(x)\sin(\omega x)\,\mathrm{d}x, \tag{21}$$

where

$$f(x) = \frac{1}{\sqrt{2\pi\sigma^2}}\mathrm{e}^{-\frac{1}{2}\left(\frac{\ln x}{\sigma}\right)^2}/x.$$

Thus, (21) is a sum $I(0) + \mathrm{j}\,I(1/2)$, where

$$I(\xi) = \int_0^\infty f(x)\sin(\omega x + \xi\pi)\,\mathrm{d}x. \tag{22}$$

The basic idea is introducing a variable transformation $x = y(t)$ so that $y(t) \to 0$ as $t \to -\infty$ and $y(t) \to \infty$ as $t \to \infty$. This introduces a factor $y'(t)$, which can be selected to enhance the rate of decay of the integrand. The transformed integral is

$$\begin{aligned}\hat{I}(\xi) &= \int_{-\infty}^\infty y'(t)f(y(t))\sin(\omega y(t) + \xi\pi)\,\mathrm{d}t \\ &= \int_{-\infty}^\infty g(t)\sin(\omega y(t) + \xi\pi)\,\mathrm{d}t,\end{aligned} \tag{23}$$

where $g(t) = y'(t)f(y(t))$. Then the integral $\hat{I}$ is approximated by a finite $2N+1$ point summation having the form

$$\hat{I}(\xi) \approx h\sum_{k=-N}^{N} g(kh)\sin\left(\pi\,\psi(kh - \xi h) + \xi\pi\right).$$

Ooura and Mori [33] cleverly select $y(t)$ such that $(\omega y(kh) + \xi\pi) \to k\pi$ as $k \to \infty$. This forces the truncation error to diminish rapidly, because the factor $\sin(\pi\psi(kh - \xi h) + \xi\pi)$ in each neglected term tends to zero for large k.

With much experimentation, they have formulated

$$\begin{aligned} y(t) &= \frac{\pi}{\omega h}\psi(t - \xi h), \\ \psi(t) &= t\left(1 - \mathrm{e}^{-(2t + \alpha(1-\mathrm{e}^{-t}) + \beta(\mathrm{e}^t - 1))}\right)^{-1}, \end{aligned}$$

where

$$\beta = \frac{1}{4}, \quad \alpha = \beta\left(1 + \frac{\log(1 + \pi/h)}{4h}\right)^{-1/2},$$

and h is the step size used in the trapezoidal rule.

The advantage of this method is that it does not use complex contour integration. However, it require careful programming to overcome underflow, overflow and unnecessary loss of precision [43]. As shown comparatively in section VI, this method too yields very high accuracy.

V. Lognormal Sum CDF

This section develops the new method to compute the SLN CDF. A 'lognormal sum' is

$$Y = \sum_{k=1}^{K} \mathrm{e}^{X_k}, \tag{24}$$

of independent lognormal random variables $X_k \sim N(\mu_k, \sigma_k^2)$. Therefore, the MGF $\mathcal{M}_Y(s)$ of Y is easily obtained by multiplying those of X_ks. The CDF of Y is thus computed by numerical Laplace inversion of $\frac{\mathcal{M}_Y(s)}{s}$.

A. Conventional approach

Conventionally, the integral (24) is evaluated over a vertical contour (known as the Bromwich contour), which passes the real axis at $x = \alpha_0, \alpha_0 \geq 0$. The accuracy is typically improved by finding through a simple search in $(0, \infty)$, the best value for α_0.

Suppose $X_k \sim N(\mu, \sigma^2)$ to be identical. The independent and non-identically distributed case as well as the non-zero mean case can be treated; but are omitted for brevity. The CDF of Y is given by

$$F(y) = \Pr[Y \leq y]. \tag{25}$$

The MGF of Y would be given by $\mathcal{M}_Y(s) = (\mathcal{M}(s))^K$, where $\mathcal{M}(s)$ is the MGF of X_k, $k = 1, \ldots, K$. It is easy to show that

$$F(y) = \int_{\alpha_0 - \mathrm{j}\infty}^{\alpha_0 + \mathrm{j}\infty} \frac{\mathcal{M}_Y(s)\,\mathrm{e}^{sy}}{2\mathrm{j}\,\pi s}\,\mathrm{d}s = \int_{\alpha_0 - \mathrm{j}\infty}^{\alpha_0 + \mathrm{j}\infty} \frac{\mathrm{e}^{\varsigma(s)}}{2\mathrm{j}\,\pi}\,\mathrm{d}s, \tag{26}$$

where $\varsigma(s) = sy + \log(\mathcal{M}_Y(s)) - \log(s)$, and α_0 is a more or less free parameter in the range $0 \leq \alpha_0 < \infty$. The reason that the Bromwich contour can be moved in this range is that the MGF is defined for all $\Re(s) \geq 0$, and no singularities of the integrand occur except at $s = 0$. Therefore, α_0 can be chosen to minimize the integrand along the real axis.

The CDF is now given by the integral

$$F(y) = \frac{1}{2\pi}\int_{-\infty}^{\infty} \frac{\mathcal{M}_Y(\alpha_0 + \mathrm{j}\,\omega)\,\mathrm{e}^{(\alpha_0 + \mathrm{j}\,\omega)y}}{\alpha_0 + \mathrm{j}\,\omega}\,\mathrm{d}\omega, \tag{27}$$

which can be evaluated by using, for example, the Gauss-Chebyshev quadrature rule. Another method is to choose $\alpha_0 = 0$ and use traditional numerical techniques (e.g., the trapezoidal rule, Simpson's rule, Clenshaw-Curtis rule) [29].

Various numerical integration techniques are available for integrating along the Bromwich contour. However, their accuracy tends to become poor, when the integrand becomes oscillatory or tends to decay slowly (this aggravates in SLN problem when the number of summands is small). Our proposed method overcomes these difficulties.

B. A novel approach

The conventional numerical solution of (27) is not accurate as y gets larger. In this case, optimal α_0, which is a function of y, tends to zero, and the integration has to be performed along a vertical line that approaches the imaginary axis. Thus, it makes sense to set $\alpha_0 = 0$, and look at a different approach. Deforming the contour (as was done in Section III) is not

possible here, because there is no analytic continuation of the lognormal MGF to the left half of the s-plane.

Therefore, we develop a different method than that using the simple numerical integration of (27). Longman [34], [35] has developed a powerful technique for the numerical evaluation of oscillating integrals. His key idea is to break down the infinite integral into a series of finite integrals, each of which is evaluated over the successive intervals between the zeros of the integrand. As a result, the integral is expressed as an alternating series, the summation of which is accelerated by Euler's transformation.

Consider the integral in (27). We set $\alpha_0 = 0$ and note that $F(y) = 0$ for $y < 0$. Thus, (27) can be simplified as

$$F(y) = \frac{2}{\pi}\int_0^\infty \frac{\Re\left(\Phi_Y(\omega)\right)\sin(\omega y)}{\omega}\,\mathrm{d}\omega,$$

where $\Phi_Y(\omega)$ is the CHF of Y. Substituting $t = \omega y$, we get

$$\begin{aligned} F(y) &= \frac{2}{\pi}\int_0^\infty \frac{\Re\left(\Phi_Y(t/y)\right)}{t}\sin t\,\mathrm{d}t \\ &= \frac{2}{\pi}\sum_{k=0}^{\infty}\int_{k\pi}^{(k+1)\pi} \frac{\Re\left(\Phi_Y(t/y)\right)}{t}\sin t\,\mathrm{d}t. \end{aligned}$$

This CDF expression can be finally obtained as

$$\begin{aligned} F(y) &= \frac{2}{\pi}\sum_{k=0}^{\infty}(-1)^k\int_0^\pi \frac{\Re\left(\Phi_Y((k\pi+t)/y)\right)}{t+k\pi}\sin t\,\mathrm{d}t \\ &= \sum_{k=0}^{\infty} a_k(-1)^k, \end{aligned} \tag{28}$$

where

$$a_k = \frac{2}{\pi}\int_0^\pi \frac{\Re\left(\Phi_Y((k\pi+t)/y)\right)}{t+k\pi}\sin t\,\mathrm{d}t. \tag{29}$$

The series expression (28) has a built-in error bound for computational purposes, because the truncation error E introduced by approximating the alternating series (28) with the partial sum of its first n terms is upper bounded as $|E| < |a_{n+1}|$. Thus, when the absolute value of the k-th term drops below the required precision level, the series can be truncated with the confidence that the truncation error is under the limit! This behavior differs from that of the conventional methods. For example, if one uses direct integration of (27), as was the case with previously published approaches, the truncation error cannot be rigorously bounded. The above approach avoids this problem.

The numerical evaluation of the k-th term a_k is quite easy because the integrand is smooth and well-behaved. Even the simple adaptive quadrature techniques available in, say, MATLAB, can reach a precision of 15 significant digits. However, (28) being a series has a serious drawback - in terms of performance (see table IV) and accuracy - if a large number of a_k's needs to be evaluated. Fortunately, convergence acceleration algorithms exist, so that a given series can be transformed into yet another series that converges faster (i.e, with a fewer number of terms, for a given precision goal) to the same limit as the original series.

Consider the partial sums $s_n = \sum_{k=0}^{n}(-1)^k a_k$ for $n = 0, 1, \ldots, N-1$. The objective is to estimate the limit s_∞ by using as few partial sums as possible. The powerful Epsilon algorithm of Shanks [36] and Wynn [37] is suitable for this purpose. The algorithm generates a two-dimensional array called the ϵ-table. In the entries $\epsilon_r^{(k)}$, subscript r is the column index and the superscript k is the location down the column. To initialize the table, the first column is set to zero as $\epsilon_{-1}^{(k)} = 0, \forall k \geq 0$ and the second column is set to the given partial sums as $\epsilon_0^{(k)} = s_k, k = 0, \ldots, N-1$. The remaining elements of the ϵ-table may be calculated from

$$\epsilon_{r+1}^{(k)} = \epsilon_{r-1}^{(k+1)} + \left[\epsilon_r^{(k+1)} - \epsilon_r^{(k)}\right]^{-1} \tag{30}$$

for $r = 1, 2, \ldots$. The even columns of the ϵ-table contains increasingly accurate estimates of $s_\infty = F(y)$ – see an example in Table I, where the first column ($r = 2$) is not convergent at all. The extrapolated values appear the columns ($r = 8$ and $r = 10$) are accurate to about 6 significant digits. This shows the extraordinary accuracy of the method because only 10 terms of (28) is required to achieve this level of accuracy.

TABLE I
EVEN COLUMNS OF THE ϵ-TABLE FOR $F(y)$ AT $y = 100$ FOR SIX I.I.D. LOGNORMAL SUMMANDS WITH $\sigma = 4\,\mathrm{dB}$

k	$r=2$	$r=4$	$r=6$	$r=8$	$r=10$
0	1.140357316				
1	0.945061679	0.995963513			
2	1.013907474	0.997596897	0.996500999		
3	0.992532962	0.993412056	0.996062704	0.996111912	
4	0.993449763	0.992411282	0.996119319	0.996108078	0.996108747
5	1.001274194	0.996695709	0.996105346	0.996108833	
6	0.990237648	0.995890592	0.996109957		
7	1.001826354	0.996209097			
8	0.990925024				

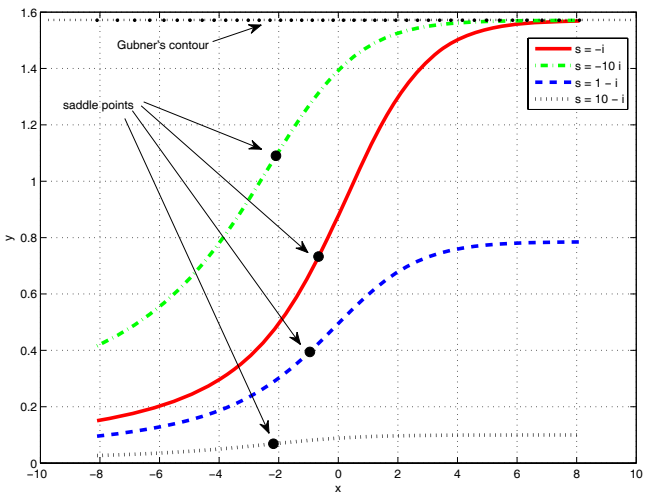

Fig. 1. Constant-phase contours to evaluate the lognormal MGF - for a lognormal RV with mean 0 dB and standard deviation 6 dB.

VI. NUMERICAL RESULTS

A. Computation of the MGF - contours

Fig. 1 shows several steepest-descent constant-phase contours (10) for a lognormal RV with mean 0 dB and standard deviation 6 dB. We use the hybrid algorithm that switches between the simple bisection algorithm and the Newton-Raphson method [42] to compute the contours (x, y) in Fig.

TABLE II
COMPARISON OF DIFFERENT CONTOURS (FOR INTEGRATION OVER CONST. PHASE, 'ATAN' AND 'TANH' CONTOURS, RESPECTIVELY, WITH 64, 128 AND 128 POINTS)

s	const. phase contour		'atan' contour		'tanh' contour	
	$\mathcal{M}(s)$	time (ms)	$\mathcal{M}(s)$	time (ms)	$\mathcal{M}(s)$	time (ms)
$-$j	0.361405531657605 +0.39181088634518j	6.7969	0.361405531657624 +0.391810886345185j	3.5312	0.361405531657624 +0.391810886345185j	3.5938
-10j	-0.0283204503044886 +0.07581405470858 27j	6.8281	-0.0283204503044922 +0.0758140547086j	3.5469	-0.0283204503044922 +0.0758140547086j	3.5938
$1-$j	0.305985649295396 +0.165599554059 96j	7.3750	0.305985649295412 +0.165599554059981j	3.9844	0.3059856492954 +0.165599554059981j	4.0781
$10-$j	0.051869201760049 +0.0064605736634504j	6.9531	0.051869201760061 1 +0.00646057366345154j	3.9219	0.051869201760061 1 +0.00646057366345154j	3.9844

TABLE III
COMPARISON OF OOURA-MORI METHOD AND STEEPEST-DESCENT INTEGRATION

σ	ω	**Ooura-Mori approach**	**contour integration**
6 dB	1	$0.361405531657622+0.391810886345190$j	$0.361405531657602+0.391810886345176$j
	10	$-0.028320450304492+0.075814054708598$j	$-0.028320450304489+0.075814054708583$j
	10^2	$-0.001832371961648-0.000326399122733$j	$-0.001832371961608-0.000326399122730$j
	10^3	$7.222777293221429\times10^{-7}-4.768704568197585\times10^{-6}$j	$7.222777286929396\times10^{-7}-4.768704563153524\times10^{-6}$j
	10^4	$1.169627421515615\times10^{-9}+2.535359603788504\times10^{-10}$j	$1.169586878600072\times10^{-9}+2.535266235219255\times10^{-10}$j
	10^5	$-8.402986648261929\times10^{-15}+2.436379811358153\times10^{-14}$j	$-4.850346982585558\times10^{-15}+1.409938611900216\times10^{-14}$j
	10^6	$-3.989622974947136\times10^{-20}-2.117359237557078\times10^{-20}$j	$-2.249403069407797\times10^{-20}-1.191840414010014\times10^{-20}$j
12dB	1	$0.420298929291493+0.214242137746210$j	$0.420298929291483+0.214242137746207$j
	10	$0.136620889892398+0.135351289903998$j	$0.136620889892397+0.135351289903997$j
	10^2	$0.020059924788571+0.043356428016001$j	$0.020059924788570+0.043356428015999$j
	10^3	$0.000316202549945+0.006839828632151$j	$0.000316202549944+0.006839828632148$j
	10^4	$-1.930070958579791\times10^{-4}+5.115996416635931\times10^{-4}$j	$-1.930070958438299\times10^{-4}+5.115996416209289\times10^{-4}$j
	10^5	$-1.673578470955915\times10^{-5}+1.688216062994716\times10^{-5}$j	$-1.673578470324281\times10^{-5}+1.688216062327433\times10^{-5}$j
	10^6	$-5.181836418281203\times10^{-7}+1.951105011584655\times10^{-7}$j	$-5.181836328384747\times10^{-7}+1.951104976897171\times10^{-7}$j
	10^7	$-6.811209556044497\times10^{-9}-5.209512195382616\times10^{-10}$j	$-6.811196135962969\times10^{-9}-5.209501196148015\times10^{-10}$j

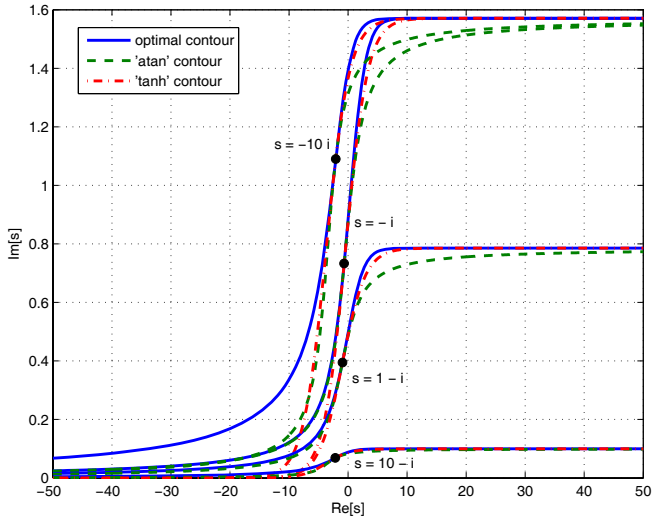

Fig. 2. A comparison of the steepest descent constant-phase, atan and tanh contours - for a lognormal RV with mean 0 dB and standard deviation 6 dB.

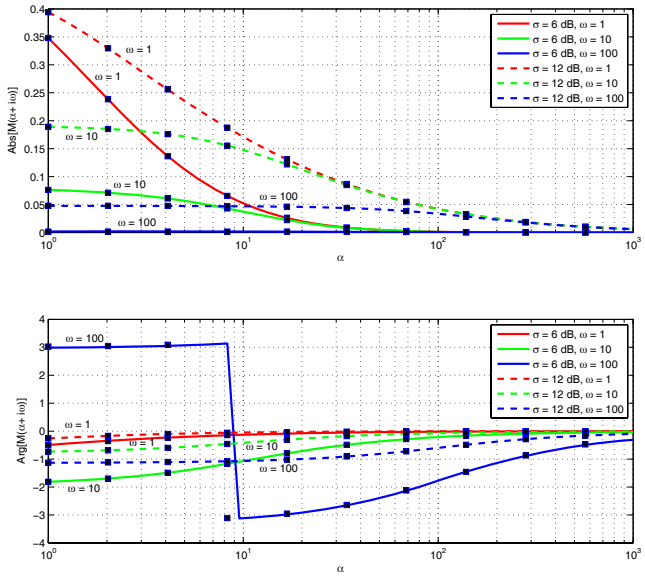

Fig. 3. Amplitude and phase of $\mathcal{M}(s)$, $s=\alpha+\mathrm{j}\,\omega$, for a lognormal RV with mean 0 dB and standard deviation σ.

1. The following trends can be noted. The optimal contours approach the real axis when $x \to -\infty$. On the other hand, as $x \to \infty$, it takes the shape of an inverse tangent function, and it always lies in the horizontal strip $0 \le y \le \pi/2$ in the x-y plane. As mentioned before, Gubner [31] suggested the contour $\mathcal{L} = \{z = x + \mathrm{j}\,\pi/2, -\infty < x < \infty\}$ for numerical evaluation of the CHF. Interestingly, a part of the optimal contour approaches Gubner's contour as $\Re(s) \to 0$ and $x \to \infty$.

In Fig. 2, the steepest-descent contour (10), the atan contour (17) and the tanh contour (20) are plotted. Both the atan and tanh contours closely track the steepest descent contour. Note that both of these are in closed-form; thus, their use reduces the computations, while retaining the benefits of the optimal contour.

Fig. 3 depicts the MGF $\mathcal{M}(s)$, $s=\alpha+\mathrm{j}\,\omega$, computed for a lognormal RV with mean 0 dB and variance σ^2. The use of the optimal contour allows the $\mathcal{M}(s)$ to be accurately computed with the simple midpoint integration rule, even for large values of the argument s. The same is possible with the atan and tanh

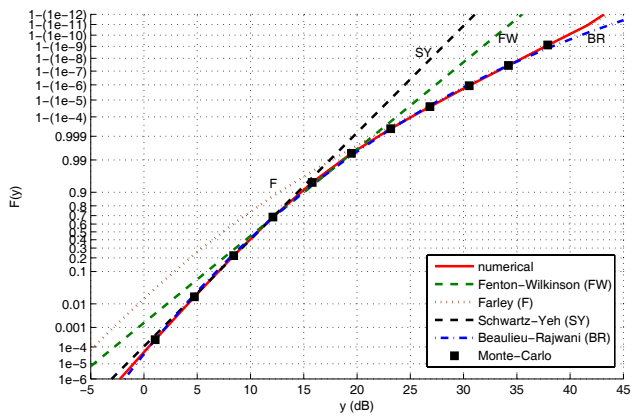

Fig. 4. The CDF of the sum of six i.i.d. lognormal RVs with mean 0 dB and standard deviation 6 dB.

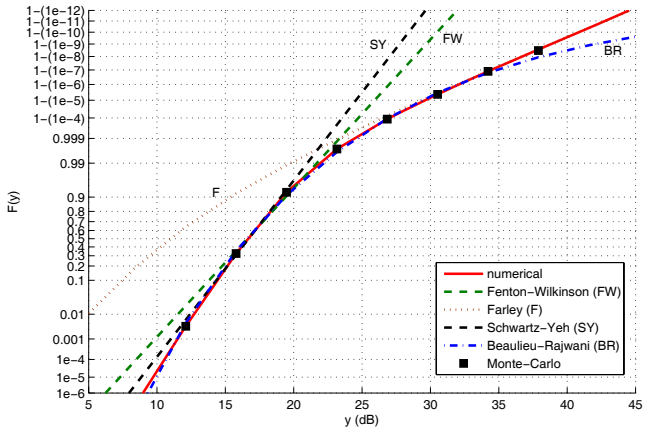

Fig. 5. The CDF of the sum of 20 i.i.d. lognormal RVs with mean 0 dB and standard deviation 6 dB.

contours as well. As expected, the amplitude of $\mathcal{M}(s)$ rapidly decays with increasing α.

In Table. II, $\mathcal{M}(s)$ values computed using the three contours and computational times are shown. Roughly, the optimal contour doubles the time of the other two contours. The optimal contour is not in closed-form and requires numerical computation via the hybrid algorithm (see III-B). All three contours agree extremely well, with the discrepancies being about 10^{-15}.

B. Computation of the MGF - contour integration vs. Ooura-Mori method

A comparison of the Ooura-Mori method and steepest-descent integration is provided in Table III. The two methods agree extremely well, with the difference being in the order of 10^{-15} and is attributable, for instance, to the rounding off errors.

C. Lognormal sum CDF

Monte Carlo simulation (with $10^{10} - 10^{11}$ sample points, depending on the required precision) is used to estimate the CDF of a sum of K lognormal RVs. The estimated CDF is used as a reference to validate our computational results. Moreover, the Fenton-Wilkinson (FW), Farley (F), Schwartz-Yeh (SY) and Beaulieu-Rajwani (BR) approximations are used for comparison purposes. Figures 4, 5 and 6 depict these results on lognormal paper [11].

Fig. 4 shows the CDF of the sum of six i.i.d. lognormal RVs with a mean 0 dB and standard deviation 6 dB. The simulations and the numerical calculations match exactly, for a wide range of y, including values as high as 45 dB (above this the Monte Carlo simulation fails to deliver sufficient accuracy). Note that apart from the BR method, the other methods fail to track the CDF accurately. The SY and FW methods fare poorly on the upper tail region, while the FW and F methods do so on the lower tail region.

The proposed algorithm based on (28) and (30) works exceptionally well, with convergence acceleration reducing the number of terms of (28) dramatically, For example, at a precision level of 10^{-15}, the number n of terms required varies from a mere 10 to 25 for the case of $\sigma \in \{6, 12\}$ dB and $0.1 < y < 10^6$. However, up to 25000000 number of terms are required when the same is attempted without acceleration. Thus, computational saving by a factor of 10^6 is possible. A timing comparison is provided in Table IV. It reveals that direct computation of (28) (at a precision level of 10^{-15}) without acceleration requires, in some cases, more than one day (estimated) to compute a single value, where as it can be computed in about 30 seconds on the same computational platform when acceleration is used.

TABLE IV
TIMING TABLE FOR EVALUATING $F(y)$ AT A PRECISION LEVEL OF 10^{-15}

σ	y	No acceleration		Epsilon method	
		# terms	time(s)	# terms	time(s)
6 dB	0.1	2	65.25	10	17.891
	1	15	72.5	15	19.422
	10	141	128.906	25	17.313
	100	672	569.437	25	22.703
	1000	6695	4643.83	25	30.047
	10000	26741	21710.6	25	33.329
	100000	$\approx$ 500000	$>$ 1 day	25	28.937
	1000000	$\approx$ 4000000		25	28.485
12 dB	0.1	35	157.14	25	27.125
	1	246	397.703	25	32.016
	10	887	1057.16	25	33.484
	100	8233	8824.69	25	31.140
	1000	67706	71168.6	25	39.125
	10000	$\approx$ 500000		25	46.125
	100000	$\approx$ 3500000	$>$ 1 day	25	44.234
	1000000	$\approx$ 25000000		25	42.671

Fig. 5 presents the CDF of the sum of 20 i.i.d. lognormal RVs with mean 0 dB and standard deviation 6 dB. The simulation and the numerical results match extremely well. Note that apart from the BR method, the other methods again fail to track the CDF accurately. The SY and FW methods fare quite poor on the upper tail region, and the FW and F methods do so on the lower tail region. Even the BR method fares poorly in the upper tail region.

Similar comparison for 4 independent but non-identical lognormal variables having mean 0 dB and respective standard deviations $6, 8, 10$ and 12 dB is made in Fig. 6. The results for the Beaulieu-Rajwani method are not presented because

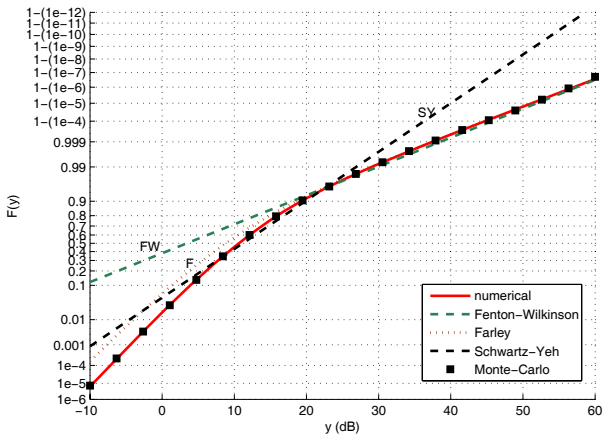

Fig. 6. The CDF of the sum of 4 independent but non-identical lognormal RVs with mean 0 dB and standard deviations $6, 8, 10$ and 12 dB respectively

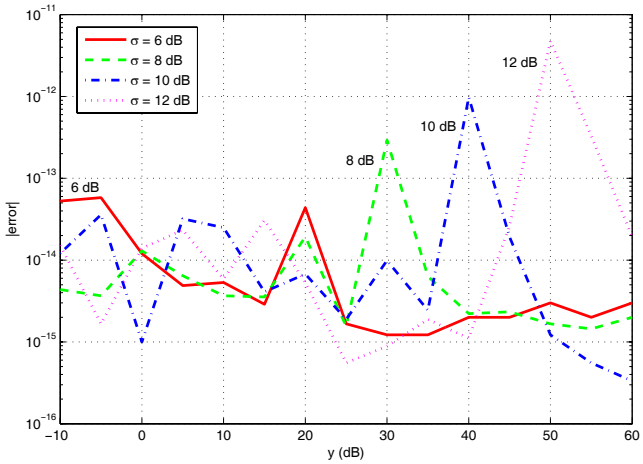

Fig. 7. Absolute Error between (28) and (31) for a single lognormal RV with mean 0 dB and standard deviation σ.

the parameters are not available for this case. Agreement with the Monte Carlo results verify the accuracy offered by the proposed scheme.

D. Verification of the accuracy

Without resorting to simulations, we can verify the accuracy of our approach for one special case. For a single lognormal RV e^Z, where $Z \sim \mathcal{N}\left(\mu, \sigma^2\right)$, the CDF is given by

$$F_Y(y) = P[\mathrm{e}^Z < y] = P[Z < \log y] = \phi\left(\frac{\log y - \mu}{\sigma}\right), \quad (31)$$

where $\phi(x)$ is the CDF of the standard normal distribution (i.e., $\mathcal{N}(0,1)$). The error is the absolute difference between (28) and (31). The CHF $\Phi_Y(\omega)$ is computed by using the steepest-descent constant-phase contour. The absolute error is plotted in Fig. 7 for σ from 6 to 12 dB. It is always less than 10^{-11}, and is less than 10^{-13} in most of the cases. This level of accuracy is, in fact, fairly close to the machine precision level. Moreover, this is the most difficult test for any lognormal sum CDF calculation algorithm because the lognormal CHF $\Phi(\omega)$ of a single lognormal RV decays slower with ω, than a product of such CHF's. Thus, as the number of summands K increases, the CHF of SLN decays more and more rapidly; and the CDF calculation becomes easier.

VII. Conclusion

This paper develops efficient, accurate computational methods for the lognormal MGF, the lognormal CHF and the SLN CDF. To overcome the highly oscillatory nature and slow decay rate of the integrands, two methods for the lognormal MGF/CHF are developed. (i.) First, we choose the constant-phase steepest-descent contour, passing through the saddle point of the integrand. Simple mid-point-rule-based integration along it computes the MGF/CHF at an accuracy about 14 to 15 significant digits. Two closed-form contours are also derived, which achieve the same level of accuracy. (ii) In the second approach, we use an ingenious transformation of Ooura and Mori [33] to derive a trapezoidal rule based computational formula for the lognormal CHF. This method also achieves the same level of accuracy. An accurate alternating series for the SLN CDF is derived, and the Epsilon algorithm is used for convergence acceleration. This acceleration dramatically reduces the computational load – sometimes by six order of magnitude. We also find that our numerical approach yields about 14 to 15 significant digits for the CDF range from 10^{-8} to $1 - 10^{-12}$. Popular approximations such as the Fenton-Wilkinson method, the Farly method and others are much less accurate in comparison. The CDF computational algorithm may also be useful in other wireless problems such as outage.

References

[1] E. Limpert, W. A. Stahel, and M. Abbt, "Log-normal distributions across the sciences: keys and clues," *BioScience*, vol. 51, no. 5, pp. 341-352, May 2001. [Online]. Available: http://www.ingentaconnect.com/content/aibs/bio/2001/

[2] J. Aitchison and J. A. C. Brown, *The Lognormal Distribution, with Special Reference to Its Uses in Economics*. Cambridge University Press, 1957.

[3] E. L. Crow and K. Shimizu, Eds., *Lognormal Distributions: Theory and Application*. CRC, 1987.

[4] G. L. Stüber, *Principles of Mobile Communication (2nd ed.)*. Norwell, MA: Kluwer Academic Publishers, 2001.

[5] C. Fischione, F. Graziosi, and F. Santucci, "Approximation for a sum of on-off lognormal processes with wireless applications," *IEEE Trans. Commun.*, vol. 55, no. 10, pp. 1984-1993, Oct. 2007.

[6] M. Pratesi, F. Santucci, and F. Graziosi, "Generalized moment matching for the linear combination of lognormal rvs: application to outage analysis in wireless systems," *IEEE Trans. Wireless Commun.*, vol. 5, no. 5, pp. 1122-1132, May 2006.

[7] M. Pratesi, F. Santucci, F. Graziosi, and M. Ruggieri, "Outage analysis in mobile radio systems with generically correlated log-normal interferers," *IEEE Trans. Commun.*, vol. 48, no. 3, pp. 381-385, Mar. 2000.

[8] C. Tellambura, "Bounds on the distribution of a sum of correlated log-normal random variables and their application," *IEEE Trans. Commun.*, vol. 56, no. 8, pp. 1241-1248, Aug. 2008.

[9] J. Zhang and V. Aalo, "Effect of macrodiversity on average-error probabilities in a Rician fading channel with correlated lognormal shadowing," *IEEE Trans. Commun.*, vol. 49, no. 1, pp. 14-18, Jan. 2001.

[10] T. Piboongungon and V. A. Aalo, "Outage probability of L-branch selection combining in correlated lognormal fading channels," *Electron. Lett.*, vol. 40, pp. 886-888, July 2004.

[11] L. Fenton, "The sum of log-normal probability distributions in scatter transmission systems," *IRE Trans. Commun. Syst.*, vol. 8, no. 1, pp. 57-67, Mar. 1960.

[12] S. C. Schwartz and Y. S. Yeh, "On the distribution function and moments of power sums with log-normal components," *Bell Syst. Tech. J.*, vol. 61, no. 7, pp. 1441-1462, 1982.

[13] D. Schleher, "Generalized Gram-Charlier series with application to the sum of log-normal variates (corresp.)," *IEEE Trans. Inf. Theory*, vol. 23, no. 2, pp. 275-280, Mar. 1977.

[14] N. Marlow, "A normal limit theorem for power sums of independent random variables," *B. S. T. J.*, vol. 46, pp. 2081-2090, Nov. 1967.

[15] I. Nasell, "Some properties of power sums of truncated normal random variables," *B. S. T. J.*, vol. 46, pp. 2091-2110, Nov. 1967.

[16] J. C. S. S. Filho, P. Cardieri, and M. D. Yacoub, "Simple accurate lognormal approximation to lognormal sums," *Electron. Lett.*, vol. 41, pp. 1016-1017, Sep. 2005.

[17] N. B. Mehta, J. Wu, A. F. Molisch, and J. Zhang, "Approximating a sum of random variables with a lognormal," *IEEE Trans. Wireless Commun.*, vol. 6, no. 7, pp. 2690-2699, July 2007.

[18] A. Ligeti, "Outage probability in the presence of correlated lognormal useful and interfering components," *IEEE Commun. Lett.*, vol. 4, no. 1, pp. 15-17, Jan. 2000.

[19] N. C. Beaulieu, A. A. Abu-Dayya, and P. J. McLane, "Estimating the distribution of a sum of independent lognormal random variables," *IEEE Trans. Commun.*, vol. 43, no. 12, p. 2869, Dec. 1995.

[20] S. Szyszkowicz and H. Yanikomeroglu, "On the tails of the distribution of the sum of lognormals," in *Proc. IEEE International Conf. Commun. ICC '07*, June 2007, pp. 5324-5329.

[21] Z. Liu, J. Almhana, and R. McGorman, "Approximating lognormal sum distributions with power lognormal distributions," *IEEE Trans. Veh. Technol.*, vol. 57, no. 4, pp. 2611-2617, July 2008.

[22] Z. Liu, J. Almhana, F. Wang, and R. McGorman, "Mixture lognormal approximations to lognormal sum distributions," *IEEE Commun. Lett.*, vol. 11, no. 9, pp. 711-713, Sept. 2007.

[23] N. C. Beaulieu and F. Rajwani, "Highly accurate simple closed-form approximations to lognormal sum distributions and densities," *IEEE Commun. Lett.*, vol. 8, no. 12, pp. 709-711, Dec. 2004.

[24] C. L. J. Lam and T. Le-Ngoc, "Estimation of typical sum of lognormal random variables using log shifted gamma approximation," *IEEE Commun. Lett.*, vol. 10, no. 4, pp. 234-235, Apr. 2006.

[25] ——, "Log-shifted gamma approximation to lognormal sum distributions," *IEEE Trans. Veh. Technol.*, vol. 56, pp. 2121-2129, July 2007.

[26] H. Nie and S. Chen, "Lognormal sum approximation with type IV Pearson distribution," *IEEE Commun. Lett.*, vol. 11, no. 10, pp. 790-792, Oct. 2007.

[27] L. Zhao and J. Ding, "Least squares approximations to lognormal sum distributions," *IEEE Trans. Veh. Technol.*, vol. 56, no. 2, pp. 991-997, Mar. 2007.

[28] ——, "A strict approach to approximating lognormal sum distributions," in *Proc. Canadian Conf. Electrical Computer Eng. CCECE '06*, May 2006, pp. 916-919.

[29] N. C. Beaulieu and Q. Xie, "An optimal lognormal approximation to lognormal sum distributions," *IEEE Trans. Veh. Technol.*, vol. 53, no. 2, pp. 479-489, Mar. 2004.

[30] A. Gil, J. Segura, and N. M. Temme, *Numerical Methods for Special Functions*. Philadelphia, PA: Society for Industrial and Applied Mathematics (SIAM), 2007.

[31] J. A. Gubner, "A new formula for lognormal characteristic functions," *IEEE Trans. Veh. Technol.*, vol. 55, no. 5, pp. 1668-1671, Sep. 2006.

[32] R. M. Corless, G. H. Gonnet, D. E. G. Hare, D. J. Jeffrey, and D. E. Knuth, "On the Lambert W function," *Adv. Comput. Math.*, vol. 5, pp. 329-359, 1996.

[33] T. Ooura and M. Mori, "A robust double exponential formula for Fourier-type integrals," *J. Comput. Appl. Math.*, vol. 112, no. 1-2, pp. 229-241, 1999, numerical evaluation of integrals.

[34] I. M. Longman, "A method for the numerical evaluation of finite integrals of oscillatory functions," *Math. Comput.*, vol. 14, pp. 53-59, 1960.

[35] ——, "Note on a method for computing infinite integrals of oscillatory functions," *Proc. Cambridge Philos. Soc.*, vol. 52, pp. 764-768, 1956.

[36] D. Shanks, "Non-linear transformations of divergent and slowly convergent sequences," *J. Math. Phys.*, vol. 34, pp. 1-42, 1955.

[37] P. Wynn, "On a device for computing the $e_m(S_n)$ tranformation," *Math. Tables Aids Comput.*, vol. 10, pp. 91-96, 1956.

[38] M. Abramowitz and I. Stegun, *Handbook of Mathematical Functions*. New York: Dover Publications, Inc., 1970.

[39] J. D. Murray, *Asymptotic Analysis*, 2nd edition, Ser. Applied Mathematical Sciences. New York: Springer-Verlag, 1984, vol. 48.

[40] C. W. Helstrom, "Evaluating the detectability of Gaussian stochastic signals by steepest descent integration," *IEEE Trans. Aerosp. Electron. Syst.*, vol. 19, no. 3, pp. 428-437, May 1983.

[41] C. W. Helstrom and J. A. Ritcey, "Evaluating radar detection probabilities by steepest descent integration," *IEEE Trans. Aerosp. Electron. Syst.*, vol. 20, no. 5, pp. 624-634, Sep. 1984.

[42] W. H. Press, S. A. Teukolsky, W. T. Vetterling, and B. P. Flannery, *Numerical Recipes*, 3rd edition. Cambridge University Press, 2007, The Art of Scientific Computing.

[43] F. Bornemann, D. Laurie, S. Wagon, and J. Waldvogel, *The SIAM 100-digit Challenge*. Philadelphia, PA: Society for Industrial and Applied Mathematics (SIAM), 2004, A Study in High-Accuracy Numerical Computing, with a foreword by David H. Bailey.

Chintha Tellambura (SM'02) received the B.Sc. degree (with first-class honors) from the University of Moratuwa, Moratuwa, Sri Lanka, in 1986, the M.Sc. degree in electronics from the University of London, London, U.K., in 1988, and the Ph.D. degree in electrical engineering from the University of Victoria, Victoria, BC, Canada, in 1993.

He was a Postdoctoral Research Fellow with the University of Victoria (1993-1994) and the University of Bradford (1995-1996). He was with Monash University, Melbourne, Australia, from 1997 to 2002. Presently, he is a Professor with the Department of Electrical and Computer Engineering, University of Alberta. His research interests include Diversity and Fading Countermeasures, Multiple-Input Multiple-Output (MIMO) Systems and Space-Time Coding, and Orthogonal Frequency Division Multiplexing (OFDM).

Prof. Tellambura is an Associate Editor for the IEEE TRANSACTIONS ON COMMUNICATIONS and the Area Editor for Wireless Communications Systems and Theory in the IEEE TRANSACTIONS ON WIRELESS COMMUNICATIONS. He was Chair of the Communication Theory Symposium in Globecom'05 held in St. Louis, MO.

Damith Senaratne (S'06) received the B.Sc. degree (with first-class honors) from the University of Moratuwa, Moratuwa, Sri Lanka, in 2005. In 2008 he received the M.Sc. degree in Telecommunications from the same university. He is currently working towards a Ph.D. degree at the Electrical and Computer Engineering Department, University of Alberta, AB, Canada. His research interests include numerical and theoretical analysis of wireless communication systems.